No. 559 **February 2017**

Natural convection flow of two-phase dusty gas with variable thermophysical properties along a vertical wavy surface

N. Begum, S. Siddiqa,
M. A. Hossain, R. S. R. Gorla

ISSN: 2190-1767

Natural convection flow of two-phase dusty gas with variable thermophysical properties along a vertical wavy surface

Naheed Begum[†], Sadia Siddiqa[*,1], Md. Anwar Hossain[‡], Rama Subba Reddy Gorla[§]

[*]*Department of Mathematics, COMSATS Institute of Information Technology, Kamra Road, Attock, Pakistan*

[†]*Institute of Applied Mathematics (LSIII), TU Dortmund, Vogelpothsweg 87, D-44221 Dortmund, Germany*

[‡]*UGC Professor, Department of Mathematics, University of Dhaka, Dhaka, Bangladesh*

[§]*Department of Mechanical Engineering, Cleveland State University, OH, USA*

Abstract: The purpose of the present study is to establish the detailed parametric solutions for laminar natural convection flow of two-phase dusty fluid moving along a vertical wavy plate. Typical sinusoidal surface is used to elucidate the heat transport phenomena for the carrier gas having variable thermophysical properties. The governing equations are cast into a system of parabolic partial differential equations by using set of continuous transformations and then the resulting system is integrated through implicit finite difference method. In order to ensure the accuracy, the present numerical results are also compared with the available published results and good compatibility is found between the present and previous results. It is showed that mass concentration parameter, D_ρ, and the variable thermophysical properties extensively promotes the rate of heat transfer near the uneven surface. It is also established that amplitude of the wavy surface enhances very drastically, which is also due to the variable properties of the fluid.

Keywords: Natural Convection, Variable Thermophysical Properties, Wavy Surface

1 Introduction

The class of problems involving the variable thermophysical properties of the fluid has attracted numerous researchers and experimentalists due to their significant applications in viscometery, food processing, instrumentation, tribology, lubrication and many others processes of engineering occurring at high temperatures. In many practical applications, these physical properties of the fluids may change significantly with temperature. For instance, the viscosity of water increases by about 240% when the temperature decreases from $500°(\mu = 0.000548 kgm^{-1}s^{-1})$ to $100°(\mu = 0.00131 kgm^{-1}s^{-1})$. In order to predict the flow behavior accurately, it is therefore important to take into the account the temperature-dependent thermophysical properties of the fluid. Until date, numerous researchers addressed the variable thermophysical properties of the fluids and reported the interesting facts on fluid flow and heat transfer. In this regard, the analysis of the variable thermophysical properties of the fluid for laminar natural convection past an isothermal vertical wall has been reported by Sparrow and Gregg [1]. In this paper, the authors presented the solutions of the boundary layer equations for some special cases. After that, Brown [2] investigated the influence of the volumetric expansion coefficient on heat transfer rate for the problem of laminar free convection. In addition, Gray and Giogini [3] discussed the

[1]Corresponding author.
Email: saadiasiddiqa@gmail.com, Ph: +923335297152

validity of the Boussinesq approximation for liquids and gases and proposed a method for analyzing natural convection flows with fluid properties. In this study, the authors assumed the physical properties of the fluid to be linear functions of temperature and pressure. It is important to mention here that, Clausing and Kempka [4] investigated the effect of variable properties on experimental basis and concluded that, for the laminar region, the rate of heat transfer Nu will be a function of Ra, only with reference temperature, T_f, which is taken as the average temperature in the boundary layer. Furthermore, the analysis of instability of laminar free convection flow and then the transition to turbulent state had been presented by Gebhart [5] and also have been summarized in a textbook by Eckert and Drake [6]. A detailed analysis of effect of variable thermophysical properties on laminar free convection of gas has also been presented in [7].

In all above-mentioned studies, attention has been given to viscous fluid which is free from all impurities (clear fluid). But, pure fluid is rarely available in many practical situations, for instance, common fluids like air and water contain impurities like dust particles. Therefore, investigations on flow of fluids with suspended particles finds its practical applications in various problem of atmospheric, engineering and physiological fields (see [9]). In this regard, Farbar and Morley [10] were the first to analyze the gas-particulate suspension on experimental grounds. After that, Marble [11] studied the problem of dynamics of a gas containing small solid particles and developed the equations for gas-particle flow systems. Singleton [12] was the first to study the boundary layer analysis for dusty fluid and later on several attempts were made to conclude the physical insight of such two-phase flows (see Ref. [13]-[19]) under different physical circumstances. Here, it is important to mention that, in all the above mentioned investigations, only the smooth surfaces were taken into account for the analysis of flow field and heat transfer. Perhaps irregular surfaces are sometimes more important in industries, for instance, solar collectors, condensers in refrigerators, cavity wall insulating systems, grain storage containers, and industrial heat radiators are a few of the many applications of rough surfaces through which small as well as the large scale heat transfer is encountered. The analysis of heat transfer along a semi-infinite vertical wavy surface of Newtonian fluid were initially discussed by Yao [20], and, after that, roughened (wavy) surfaces, have been extensively used in the literature (see Ref. [21]-[28]) under several different circumstances. After that, Siddiqa *et al.* ([29]-[30]) was the first to exploit the rough surfaces for the analysis of heat transfer in dusty fluid flow. In these papers, the author reported significant effects of surface non-uniformities for the natural convection of air and water particulate suspensions.

It is found that the problem of natural convection flow of two-phase dusty fluid with variable thermophysical properties along a vertical wavy surface has not been treated in the literature. It is, therefore, the purpose of the present study to report the influence of surface waviness on natural convection boundary layer flow of the two-phase dusty fluid having temperature dependent thermophysical properties. It is assumed that the influence of variable properties of the carrier fluid is confined into the region near the wavy geometry and remains uniform in the main stream. Taking Grashof number Gr to be very large, the boundary layer approximation is invoked leading to a set of non-similar parabolic partial differential equations whose solution is obtained through implicit finite difference method. From the present analysis, we will interrogate whether i) the roughness element ii) the presence of dust particles in base fluid and iii) variable thermophysical properties of the carrier fluid, affect the natural convection and alter the physical characteristics associates

with the vertical wall or not? Therefore, interaction of combined effect of wavy surface, dust-particles and variable thermophysical properties of carrier phase presents an interesting fluid dynamics problem. The computational results are presented graphically in the form of wall shear stress, heat transfer rate, velocity and temperature profiles by varying important controlling parameters.

2 Problem Formulation

A two-dimensional natural convection flow of two-phase dusty fluid is modeled along a vertical wavy surface. In the analysis, consideration have been to variable thermophysical properties of steady, viscous and incompressible carrier fluid containing the dust particles. The physical model and the coordinate system used for natural convection along an isothermal vertical wavy plate is shown in Fig. 1. The boundary layer analysis outlined below allows the shape of the wavy surface, $y_w = \sigma(x)$, to be arbitrary, but our detailed numerical work will assume that the surface exhibits sinusoidal deformations. In particular, we assume that the surface profile is given by:

$$y_w = \sigma(x) = a \sin\left(\frac{2\pi x}{L}\right) \tag{1}$$

where a represents the amplitude of the transverse surface wave and L the characteristic length associated with the wave. Both the gas and the particle cloud along the vertical wavy surface are supposed to be static at the beginning and the number density of the particles is taken as uniform throughout the flow. Assumption is being made that the dust particles in carrier fluid are spherical in shape and uniform in size so that the conservation equations given by Saffman [14] remains valid. The equations describing the convective flow of two-phase dusty fluid along the vertical surface can be written in dimensional form as follows (For details see [14], [19]):
For gas phase:

$$\frac{\partial(\rho u)}{\partial x} + \frac{\partial(\rho v)}{\partial y} = 0 \tag{2}$$

$$\rho\left(u\frac{\partial u}{\partial x} + v\frac{\partial u}{\partial y}\right) = -\frac{\partial p}{\partial x} + \mu\left(\frac{\partial^2 u}{\partial x^2} + \frac{\partial^2 u}{\partial y^2}\right) + \frac{\partial \mu}{\partial x}\frac{\partial u}{\partial x} + \frac{\partial \mu}{\partial y}\frac{\partial u}{\partial y} + \frac{\rho g\,(T - T_\infty)}{T_\infty} + \frac{\rho_p}{\tau_m}(u_p - u) \tag{3}$$

$$\rho\left(u\frac{\partial v}{\partial x} + v\frac{\partial v}{\partial y}\right) = -\frac{\partial p}{\partial y} + \mu\left(\frac{\partial^2 v}{\partial x^2} + \frac{\partial^2 v}{\partial y^2}\right) + \frac{\partial \mu}{\partial x}\frac{\partial v}{\partial x} + \frac{\partial \mu}{\partial y}\frac{\partial v}{\partial y} + \frac{\rho_p}{\tau_m}(v_p - v) \tag{4}$$

$$\rho c_p\left(u\frac{\partial T}{\partial x} + v\frac{\partial T}{\partial y}\right) = \frac{\partial}{\partial x}\left(\kappa\frac{\partial T}{\partial x}\right) + \frac{\partial}{\partial y}\left(\kappa\frac{\partial T}{\partial y}\right) + \frac{\rho_p c_s}{\tau_T}(T_p - T) \tag{5}$$

For the particle phase:

$$\frac{\partial u_p}{\partial x} + \frac{\partial v_p}{\partial y} = 0 \tag{6}$$

$$\rho_p\left(u_p\frac{\partial u_p}{\partial x} + v_p\frac{\partial u_p}{\partial y}\right) = -\frac{\partial p_p}{\partial x} - \frac{\rho_p}{\tau_m}(u_p - u) \tag{7}$$

$$\rho_p\left(u_p\frac{\partial v_p}{\partial x} + v_p\frac{\partial v_p}{\partial y}\right) = -\frac{\partial p_p}{\partial y} - \frac{\rho_p}{\tau_m}(v_p - v) \tag{8}$$

$$\rho_p c_s \left(u_p \frac{\partial T_p}{\partial x} + v_p \frac{\partial T_p}{\partial y} \right) = -\frac{\rho_p c_s}{\tau_T}(T_p - T) \tag{9}$$

where (u, v), T, p, ρ, c_p, κ and μ are respectively the velocity vector in the (x, y) direction, temperature, pressure, density, specific heat at constant pressure, thermal conductivity and the dynamic viscosity of the fluid/carrier phase. Similarly, (u_p, v_p), T_p, p_p, ρ_p and c_s corresponds to the velocity vector, temperature, pressure, density and specific heat for the particle phase, respectively. Likewise, g is the gravitational acceleration, τ_m (τ_T) is the momentum relaxation time (thermal relaxation time) during which the velocity (temperature) of the particle phase relative to the fluid is reduced to $1/e$ times its initial value.

The fundamental equations stated above are to be solved under appropriate boundary conditions to determine the flow fields of the gas and the dust particles. Therefore, the boundary conditions for the problem under considerations are:
For gas phase:

$$\begin{gathered} u(x, y_w) = v(x, y_w) = T(x, y_w) - T_w = 0 \\ u(x, \infty) = T(x, \infty) - T_\infty = 0 \end{gathered} \tag{10}$$

For the particle phase:

$$\begin{gathered} u_p(x, y_w) = v_p(x, y_w) = T_p(x, y_w) - T_w = 0 \\ u_p(x, \infty) = T_p(x, \infty) - T_\infty = 0 \end{gathered} \tag{11}$$

where T_∞ symbolize the ambient carrier fluid temperature such that $T_w >> T_\infty$.

There are very few forms of temperature-dependent thermophysical properties of the fluids available in the literature. Among them, we have considered that ones which are appropriate for the class of gases introduced by ([7], [8]) and mathematically can be expressed as follows:

$$\mu/\mu_\infty = (T/T_\infty)^{n_\mu}, \quad \kappa/\kappa_\infty = (T/T_\infty)^{n_\lambda} \tag{12}$$

while the variation in density and kinematic viscosity with thermodynamic temperature at uniform pressure are assumed as:

$$\rho/\rho_\infty = (T/T_\infty)^{-1}, \quad \nu/\nu_\infty = (T/T_\infty)^{n_\mu + 1} \tag{13}$$

where, $\mu_\infty(\nu_\infty)$, ρ_∞ and κ_∞ are respectively, the dynamic (kinematic) viscosity, the density and the thermal conductivity of the carrier fluid in the free-stream region. Furthermore, the values of n_μ and n_λ are taken from the analysis of Hisenrath *et al.* [8], which is based on the summarized experimental values of μ and κ for several monoatomic and diatomic gases, and also for air and water vapours. Besides, it is important to mention here that, the thermodynamic temperature of the fluid away from the wavy surface of the plate, T_∞, is taken as the reference temperature for the analysis of natural convection.

Now, by following Yao [20], the following dimensionless variables are introduced for non-dimensionalization of the governing equations:

$$\begin{gathered} X = \frac{x}{L}, \quad Y = \frac{y - \sigma(x)}{L} Gr^{1/4}, \quad (u, u_p) = \frac{\nu_0}{L} Gr^{1/2}(U, U_p), \\ (\theta, \theta_p) = \frac{(T, T_p) - T_\infty}{T_w - T_\infty}, \quad (v, v_p) = \frac{\nu_0}{L} Gr^{1/4} \Big((V, V_p) + \sigma_x Gr^{1/4}(U, U_p) \Big), \\ (P, P_p) = \frac{L^2}{\rho \nu_0^2 Gr}(p, p_p), \quad \lambda = \frac{T_w - T_\infty}{T_\infty}, \quad Gr = \frac{g(T_w - T_\infty)L^3}{\nu^2} \end{gathered} \tag{14}$$

Upon introducing the dimensionless variables (14) into the Eqs. (1)-(13), the following dimensionless form of the governing equations are obtained at leading order in the Grashof number, Gr:
For gas phase:

$$\frac{\partial U}{\partial X}+\frac{\partial V}{\partial Y}+\frac{1}{\rho}\left(U\frac{\partial \rho}{\partial X}+V\frac{\partial \rho}{\partial Y}\right)=0 \tag{15}$$

$$U\frac{\partial U}{\partial X}+V\frac{\partial U}{\partial Y}=-\frac{\partial P}{\partial X}+\sigma_X Gr^{1/4}\frac{\partial P}{\partial Y}+\frac{\nu}{\nu_0}(1+\sigma_X^2)\left(\frac{\partial^2 U}{\partial Y^2}+\frac{1}{\mu}\frac{\partial \mu}{\partial Y}\frac{\partial U}{\partial Y}\right)+\theta +D_\rho\alpha_d(U_p-U) \tag{16}$$

$$\sigma_X\left(U\frac{\partial U}{\partial X}+V\frac{\partial U}{\partial Y}\right)+\sigma_{XX}U^2=-Gr^{1/4}\frac{\partial P}{\partial Y}+\frac{\nu}{\nu_0}\sigma_X(1+\sigma_X^2)\left(\frac{\partial^2 U}{\partial Y^2}+\frac{1}{\mu}\frac{\partial \mu}{\partial Y}\frac{\partial U}{\partial Y}\right) +\sigma_X D_\rho\alpha_d(U_p-U) \tag{17}$$

$$\frac{\nu_0}{\nu}\left(U\frac{\partial \theta}{\partial X}+V\frac{\partial \theta}{\partial Y}\right)=\frac{(1+\sigma_X^2)}{\mathrm{Pr}}\left(\frac{\partial^2 \theta}{\partial Y^2}+\frac{1}{\kappa}\frac{\partial \kappa}{\partial Y}\frac{\partial \theta}{\partial Y}\right)+\frac{2}{3\mathrm{Pr}}D_\rho\alpha_d(\theta_p-\theta) \tag{18}$$

For particle phase:

$$\frac{\partial U_p}{\partial X}+\frac{\partial V_p}{\partial Y}=0 \tag{19}$$

$$U_p\frac{\partial U_p}{\partial X}+V_p\frac{\partial V_p}{\partial Y}=-\frac{\partial P_p}{\partial X}+\sigma_X Gr^{1/4}\frac{\partial p_p}{\partial Y}-\alpha_d(U_p-U) \tag{20}$$

$$\sigma_X\left(U_p\frac{\partial U_p}{\partial X}+X_p\frac{\partial U_p}{\partial Y}\right)+U_p^2\sigma_{XX}=-Gr^{1/4}\frac{\partial P_p}{\partial Y}-\alpha_d\sigma_X(U_p-U) \tag{21}$$

$$U_p\frac{\partial \theta_p}{\partial X}+V_p\frac{\partial \theta_p}{\partial y}=-\frac{2}{3\gamma\mathrm{Pr}}\alpha_d(\theta_p-\theta) \tag{22}$$

where, Gr and Pr are respectively the dimensionless Grashof number and Prandtl number. The carrier phase and particle phase are interacted through the terms: γ, D_ρ, τ_T and α_d. Particularly, $\gamma(=c_s/c_p)$ is the specific heat ratio of the mixture. For different gas-particle combinations, γ may vary between 0.1 and 10.0, and in such cases, either the temperature or the velocity tends to reach equilibrium faster (see [9]). $D_\rho(=\rho_p/\rho)$ is the mass concentration of particle phase or the ratio of densities of the fluid and the dust particles. $\tau_T=1.5\gamma\tau_m Pr$ is the relation between thermal relaxation time (τ_T) and velocity relaxation time (τ_m); indicating that τ_T is obeying the Stokes law. Finally, $\alpha_d=L^2/\nu\tau_m Gr^{1/2}$ is the parameter depending on the relaxation time of the particles and the buoyancy force.

As it can be noted form Eq. (16) that the pressure gradient is of order $O(Gr^{-1/4})$ along the normal Y direction, which implies that the lower order of pressure gradient along X direction can be determined from the inviscid flow solution. However, due to the fact that there is no externally induced free stream, this pressure gradient is taken as zero, i.e, $\partial P/\partial X=0$. Furthermore, Eq. (16) indicates that the term $Gr^{1/4}\partial P/\partial Y$ is of O (1) and can be determined by the left-hand side of this equation. Thus by eliminating the term $\partial P/\partial Y$ form Eqs. (16) and (17), we will have the following form of momentum equation:

$$\frac{\nu_0}{\nu}\left(U\frac{\partial U}{\partial X}+V\frac{\partial U}{\partial Y}+\frac{\sigma_X\sigma_{XX}}{(1+\sigma_X^2)}U^2-\frac{\theta}{(1+\sigma_X^2)}-D_\rho\alpha_d(U_p-U)\right)=(1+\sigma_X^2)\left(\frac{\partial^2 U}{\partial Y^2} +\frac{1}{\mu}\frac{\partial \mu}{\partial Y}\frac{\partial U}{\partial Y}\right) \tag{23}$$

The same reason holds for dusty phase and the elimination of $\partial P_p/\partial Y$ form Eqs. (20) and (21), leads to:

$$U_p\frac{\partial U_p}{\partial X}+V_p\frac{\partial U_p}{\partial Y}+\frac{\sigma_X\sigma_{XX}}{\left(1+\sigma_X^2\right)}U_p^2=-D_\rho\alpha_d\left(U_p-U\right) \tag{24}$$

The dimensionless form of the boundary conditions for present analysis is:
For gas phase:

$$\begin{gathered}U(X,0)=V(X,0)=\theta(X,0)-1=0\\U(X,\infty)=\theta(X,\infty)=0\end{gathered} \tag{25}$$

For particle phase:

$$\begin{gathered}U_p(X,0)=V_p(X,0)=\theta_p(X,0)-1=0\\U_p(X,\infty)=\theta_p(X,\infty)=0\end{gathered} \tag{26}$$

Now we propose to integrate the above system of equations for two-phase model. But, before applying the numerical scheme, these equations are transformed to suitable form with the help of primitive variable formulations. To establish the solutions of the above coupled equations, we switch into another system of equations with the help of following set of continuous transformations:

$$X=\xi,\quad Y=X^{\frac{1}{4}}\eta,\quad (U,U_p)=X^{\frac{1}{2}}(\overline{U},\overline{U}_p),\quad (V,V_p)=X^{-\frac{1}{4}}(\overline{V},\overline{V}_p),\quad (\theta,\theta_p)=(\Theta,\Theta_p) \tag{27}$$

The equations (15), (18), (19) (22), (23) and (24) subject to the boundary conditions (25)-(26) will be mapped into the following system of parabolic partial differential equations (after dropping bars):
For gas phase:

$$\frac{1}{2}U+\xi\frac{\partial U}{\partial\xi}-\frac{1}{4}\eta\frac{\partial U}{\partial\eta}+\frac{\partial V}{\partial\eta}+\frac{1}{\rho}\left(\xi U\frac{\partial\rho}{\partial\xi}+\left(V-\frac{1}{4}\eta U\right)\frac{\partial\rho}{\partial\eta}\right)=0 \tag{28}$$

$$\frac{\nu_0}{\nu}\left[\left(\frac{1}{2}+\frac{\xi\sigma_\xi\sigma_{\xi\xi}}{(1+\sigma_\xi^2)}\right)U^2+\xi U\frac{\partial U}{\partial\xi}+\left(V-\frac{1}{4}\eta U\right)\frac{\partial U}{\partial\eta}-\frac{\Theta}{(1+\sigma_\xi^2)}-D_\rho\alpha_d\xi^{1/2}(U_p-U)\right]=$$
$$(1+\sigma_\xi^2)\left(\frac{\partial^2U}{\partial\eta^2}+\frac{1}{\mu}\frac{\partial\mu}{\partial\eta}\frac{\partial U}{\partial\eta}\right) \tag{29}$$

$$\frac{\nu_0}{\nu}\left[\xi U\frac{\partial\Theta}{\partial\xi}+\left(V-\frac{1}{4}\eta U\right)\frac{\partial\Theta}{\partial\eta}\right]=\frac{(1+\sigma_\xi^2)}{\mathrm{Pr}}\left(\frac{\partial^2\Theta}{\partial\eta^2}+\frac{1}{\kappa}\frac{\partial\kappa}{\partial\eta}\frac{\partial\Theta}{\partial\eta}\right)+\frac{2}{3\mathrm{Pr}}D_\rho\alpha_d\xi^{1/2}(\Theta_p-\Theta) \tag{30}$$

From equations (12)-(13) combined with equations (14) and (27), we have:

$$\frac{1}{\rho}\frac{\partial\rho}{\partial\eta}=-\frac{\lambda}{(1+\lambda\Theta)}\frac{\partial\Theta}{\partial\eta},\quad \frac{1}{\rho}\frac{\partial\rho}{\partial\xi}=-\frac{\lambda}{(1+\lambda\Theta)}\frac{\partial\Theta}{\partial\xi} \tag{31}$$

$$\frac{1}{\rho}\frac{\partial\mu}{\partial\eta}=\frac{\lambda n_\mu}{(1+\lambda\Theta)}\frac{\partial\Theta}{\partial\eta},\quad \frac{1}{\rho}\frac{\partial\kappa}{\partial\eta}=\frac{\lambda n_\lambda}{(1+\lambda\Theta)}\frac{\partial\Theta}{\partial\eta} \tag{32}$$

and

$$\frac{\nu_0}{\nu}=(1+\lambda\Theta)^{-(1+n_\mu)} \tag{33}$$

where, $\lambda = (T_w - T_\infty)/T_\infty$. Now by incorporating the equations form (31)-(33) in the system of equations (28)-(30), we will have:
For gas phase:

$$\frac{1}{2}U + \xi\frac{\partial U}{\partial \xi} - \frac{1}{4}\eta\frac{\partial U}{\partial \eta} + \frac{\partial V}{\partial \eta} - \frac{\lambda}{(1+\lambda\Theta)}\left(\xi U\frac{\partial \Theta}{\partial \xi} + \left(V - \frac{1}{4}\eta U\right)\frac{\partial \Theta}{\partial \eta}\right) = 0 \tag{34}$$

$$\begin{aligned}(1+\lambda\Theta)^{-(1+n_\mu)}\left[\left(\frac{1}{2} + \frac{\xi\sigma_\xi\sigma_{\xi\xi}}{(1+\sigma_\xi^2)}\right)U^2 + \xi U\frac{\partial U}{\partial \xi} + \left(V - \frac{1}{4}\eta U\right)\frac{\partial U}{\partial \eta} - \frac{\Theta}{(1+\sigma_\xi^2)}\right.\\ \left. -D_\rho\alpha_d\xi^{1/2}(U_p - U)\right] = (1+\sigma_\xi^2)\left(\frac{\partial^2 U}{\partial Y^2} + \frac{\lambda n_\mu}{(1+\lambda\Theta)}\frac{\partial \Theta}{\partial \eta}\frac{\partial U}{\partial \eta}\right)\end{aligned} \tag{35}$$

$$\begin{aligned}(1+\lambda\Theta)^{-(1+n_\mu)}\left[\xi U\frac{\partial \Theta}{\partial \xi} + \left(V - \frac{1}{4}\eta U\right)\frac{\partial \Theta}{\partial \eta}\right] = \frac{(1+\sigma_\xi^2)}{\mathrm{Pr}}\left(\frac{\partial^2 \Theta}{\partial Y^2} + \frac{\lambda n_\lambda}{(1+\lambda\Theta)}\left(\frac{\partial \Theta}{\partial \eta}\right)^2\right)\\ +\frac{2}{3\mathrm{Pr}}D_\rho\alpha_d\xi^{1/2}(\Theta_p - \Theta)\end{aligned} \tag{36}$$

For the particle phase:

$$\frac{1}{2}U_p + \xi\frac{\partial U_p}{\partial \xi} - \frac{1}{4}\eta\frac{\partial U_p}{\partial \eta} + \frac{\partial V_p}{\partial \eta} = 0 \tag{37}$$

$$\left(\frac{1}{2} + \frac{\xi\sigma_\xi\sigma_{\xi\xi}}{\left(1+\sigma_\xi^2\right)}\right)U_p^2 + \xi U_p\frac{\partial U_p}{\partial \xi} + \left(V_p - \frac{1}{4}\eta U_p\right)\frac{\partial U_p}{\partial \eta} = -\alpha_d\xi^{1/2}(U_p - U) \tag{38}$$

$$\xi U_p\frac{\partial \Theta_p}{\partial \xi} + \left(V_p - \frac{1}{4}\eta U_p\right)\frac{\partial \Theta_p}{\partial \xi} = -\frac{2}{3\gamma\mathrm{Pr}}\alpha_d\xi^{1/2}\left(\Theta_p - \Theta\right) \tag{39}$$

subject to the boundary conditions:

$$\begin{aligned}U(\xi,0) = U_p(\xi,0) = V(\xi,0) = V_p(\xi,0) = \Theta(\xi,0) - 1 = \Theta_p(\xi,0) - 1 = 0\\ U(\xi,\infty) = U_p(\xi,\infty) = \Theta(\xi,0) = \Theta_p(\xi,0) = 0\end{aligned} \tag{40}$$

A numerical solution for the coupled system of non linear partial differential Eqs. (34)-(40) by a finite difference method is straightforward, since the computational grids can be fitted to the body shape in (ξ, η) coordinates. The discretization process is carried out by exploiting the central difference quotients for diffusion terms, and the forward difference for the convection terms. The computational process is started at $\xi = 0.0$ as the singularity at this point has been removed by the scaling. At every ξ station, the computations are iterated until the difference of the results, of two successive iterations become less or equal to 10^{-6}. In order to get accurate results, we have compared the results at different grid size in η direction and reached at the conclusion to chose $\Delta\eta = 0.003$. In this integration, the maximum value of η is taken to be 50.0. A detail description of discretization procedure and numerical scheme is presented in [28].
At this position, the skin friction coefficient and the rate of heat transfer can be calculated which are important physical quantities from engineering point of view. The mathematical

relations for these quantities are:

$$\begin{aligned} \tau_w = C_f \left(\frac{Gr^{-3}}{\xi}\right)^{1/4} &= (1+\lambda)^{-(n_\mu+1)}\sqrt{1+\sigma_\xi^2}\left(\frac{\partial U}{\partial \eta}\right)_{\eta=0} \\ Q_w = Nu\left(\frac{Gr}{\xi}\right)^{-1/4} &= -(1+\lambda)^{n_\lambda}\sqrt{1+\sigma_\xi^2}\left(\frac{\partial \Theta}{\partial \eta}\right)_{\eta=0} \end{aligned} \tag{41}$$

Now the numerical results obtained for the key parameters are discussed in the section below.

3 Results and Discussion

The main purpose of present study is to investigate the influence of variable thermophysical properties on natural convection flow of two-phase dusty gas past a vertical wavy surface. We performed two-dimensional simulations in order to obtain solutions of mathematical model presented in terms of primitive variables given in Eqs. (34)-(40) from the two-point implicit finite difference method. Numerical results are reported for the overall effectiveness of thermophysical properties parameters and the mass concentration of dust particles in fluid which is moving along a transverse geometry. As the influence of dust loading parameters and the temperature dependent properties is more pronounced for gases, therefore, present numerical solutions are performed for dusty air (i.e, Pr = 0.7, $D_\rho = 10000.0$ and $\gamma = 0.45$) with variable properties (i.e., $n_\mu = 0.68, n_\lambda = 0.81, \lambda = 1.0$). The parametric values for dust parameters are taken from study of Apazidis [31], whereas the values of variable properties are taken from the analysis of Shang and Wang [7]. During the computations, the values of the other parameters are set as: $a = (0.0, 0.1, 0.3)$ and $\alpha_d = 1.0$.

In order to validate the accuracy of our scheme and numerical computations, comparison is also being made with already published articles. It is noteworthy to mention here that a number of investigations can be retrieved that are discussed in the literature by various authors. Specifically for $a = D_\rho = \alpha_d = 0.0$, the analysis of Shang and Wang [7] becomes the special case of the present analysis. A comparison for numerical values of rate of heat transfer, $-(\partial\Theta/\partial\eta)_{\eta=0}$, for some gases is presented in Table 1. The code is further tested by comparing solutions in tabular form, with one of the study of Siddiqa *et al.* [19], which was done for smooth plate problem (see Table 2). These results are obtained by setting ($n_\mu = n_\lambda = \lambda = 1.0$) along a flat surface $a = 0.0$ for $D_\rho = (0.0, 5.0)$, Pr = 0.005 and $\gamma = \alpha_d = 1.0$. It is observed from the table that the computational values show good comparison between the studies. In addition, the solutions obtained by Yao [20] can be recovered by setting $a = 0.1, 0.3$, Pr = 1.0, ($n_\mu = n_\lambda = \lambda = 1.0$), $\alpha_d = 0.0$ and $D_\rho = 0.0$. This comparison is appeared in Fig. 2. In reference [20], stream function formulation have been used and solution are presented via Keller box method, while on the other hand, present authors adopted the primitive variable formulation and solved the problem via Thomas algorithm. It is shown that, both results match well with each other, which validate the accuracy and convergence of our numerical results (see Fig. 2).

Graphical presentation of skin friction coefficient, τ_w, and rate of heat transfer coefficient, Q_w for air particulate suspension is given in Fig. 3. For comparison, the air is taken with uniform as well as variable thermophysical properties. As it can be noted form Fig. 3(a), that the skin friction coefficient for i) air with uniform thermophysical

Table 1: The comparison between calculated values of $-(\partial\Theta/\partial\eta)_{\eta=0}$ and those reported in Ref. [7].

T_w/T_∞	Ar Pr = 0.622 $n_\mu = 0.72$ $n_\lambda = 0.73$		H_2 Pr = 0.68 $n_\mu = 0.68$ $n_\lambda = 0.8$		Air Pr = 0.7 $n_\mu = 0.68$ $n_\lambda = 0.81$	
	Ref. [7]	Present	Ref. [7]	Present	Ref. [7]	Present
3	0.1940	0.19388	0.1974	0.19736	0.1987	0.19868
5/2	0.2256	0.22559	0.2300	0.22995	0.2316	0.23160
2	0.2714	0.27133	0.2772	0.27719	0.2794	0.27938
3/2	0.3438	0.34375	0.3526	0.35254	0.3557	0.35568
5/4	0.3990	0.39902	0.4105	0.41045	0.4188	0.41878
1/2	0.8334	0.83483	0.8774	0.87793	0.8898	0.89027

Table 2: The comparison between calculated values of τ_w and Q_w with those reported in Ref. [19] for $D_\rho = (0.0, 5.0)$, Pr = 0.005, $a = \lambda = n_\lambda = n_\mu = 0.0$ and $\gamma = \alpha_d = 1.0$.

ξ	τ_w		Q_w		τ_w		Q_w	
	$D_\rho = 0.0$				$D_\rho = 5.0$			
	Ref. [19]	Present	Ref. [19]	Present	Ref. [19]	Present	Ref. [19]	Present
1.0	1.42523	1.42742	0.04170	0.04097	0.96330	0.96201	0.06391	0.06396
2.0	1.42523	1.42742	0.04170	0.04097	0.93821	0.94802	0.06398	0.06398
5.0	1.42523	1.42742	0.04170	0.04097	0.92274	0.93503	0.06401	0.06399
6.0	1.42523	1.42742	0.04170	0.04097	0.92100	0.93304	0.06402	0.06399
7.0	1.42523	1.42742	0.04170	0.04097	0.91976	0.93149	0.06402	0.06399
9.0	1.42523	1.42742	0.04170	0.04097	0.91809	0.92923	0.06402	0.06399
10.0	1.42523	1.42742	0.04170	0.04097	0.91751	0.92835	0.06402	0.06399

properties, and ii)air with uniform thermophysical properties, decreases when the value of mass concentration parameter D_ρ increases from 0.0 to 10^2. The carrier phase loses some kinetic energy from the particles through the interaction and as a result the velocity gradient for the carrier fluid decreases at the surface. In addition, it can also be visualize that the τ_w shows a clear decline when the thermophysical properties of the air suspension are taken as temperature dependent. Specifically, this reduction of τ_w is more pronounced for pure air (i.e, $D_\rho = 0.0$). On the contrary, rate of heat transfer coefficient drastically increases (see Fig. 3(b)). It is worthy to mention here that Q_w is mainly influenced due to particle impingement on the sediment layer. For higher values of D_ρ, the dusty air gains the kinetic and thermal energy from the particles and the relative velocity of particle phase increases and the particles moves through the thermal boundary layer region with less time, thus preserving the lower temperature of the regions away from the interface. This tends to increase the temperature gradient between the impinging particles and the sediment and consequently the rate of heat transfer coefficient is promoted. Interestingly, it is also recorded from Fig. 3(b), that the variable thermpophyical properties only influence the dusty air, as the plot are identical for pure air with uniform and variable thermpophyical

properties.

The numerical values of τ_w and Q_w for some values of amplitude of the wavy cone parameter, a, is presented through Fig. 4. The results for $a = 0.0$ are those which are valid for the purely vertical wall problem. Therefore, for $a = 0.0$ the waviness of the surface disappears and the numerical values shows the solution of natural convection of dusty fluid with variable thrmophysical properties over a smooth wall. As a whole, both physical quantities decreases sufficiently when the amplitude of the sinusoidal waveform increases. The reduction in the magnitude of the temperature gradient happened due to the simultaneous influence of centrifugal and buoyancy forces. Highest steeper peak points are found near the vicinity of the wavy surface. For instance, the reason for such behavior of Q_w is due to the fact that, the magnitude of the local heat transfer rate near the vicinity of the vertical plate depends on the slope of the wavy surface, so it is mainly controlled by the stream motion induced by the buoyancy force parallel to the geometry. Downstream Q_w varies according to the orientation of the surface. For the portion of the wavy surface parallel to the gravitational force, the velocity is larger and so is the heat transfer rate. The wavelength of the local heat transfer rate is half of that of the wavy surface. The peak of the heat transfer rate after one wavelength from the leading edge is shifted slightly upstream from the trough and the crest due to the convection effect. The magnitude of the variation of the heat transfer rate decreases downstream as expected, since the natural convection boundary layer grows thick. The wavy surface effect in a viscous layer is mainly due to the diffusion process. This effect becomes small when the amplitude of the wavy surface is completely covered in the boundary layer. Such characteristics of Q_w validates the results reported by Yao [20].

Fig. 5 is plotted, to make the comparison of skin friction coefficients and rate of heat transfer for two different particulate suspension of gases. The numerical computations are performed for practical examples, such that, i) air ($\Pr = 0.7, n_\mu = 0.68, n_\lambda = 0.81$), and ii) O_2($\Pr = 0.733, n_\mu = 0.694, n_\lambda = 0.86$) and these values are taken from the study of Shang and Wang [7]. It is observed from Fig. 5, that the skin friction coefficient and the rate of heat transfer are same for pure air and O_2 (i.e, $D_\rho = 0.0$), but shows a pronounced change when these gases are contaminated with dust particles. It is noted from Fig. 5(a) that, comparatively, the skin friction is minimum for air particulate suspension. Since the air is composition of all raw gases, therefore, τ_w is too low for the case of air, whereas, its shows its higher value for O_2. On the other hand, reverse behavior is recoded in rate of heat transfer Q_w (see Fig. 5(b)). The rate of heat transfer is maximum for air and decreases when the O_2 are penetrated into the mechanism. It is important to mention here that, not only the magnitude of Q_w increases for dusty air but also the amplitude of the pure sinusoidal waveform get intensified. The entire convective regime is hotter for the case of air and the large temperature gradient in the thermal boundary layer promotes conductive heating near the surface of the plate.

The influence of variable thermophysical properties on skin friction coefficient and rate of heat transfer for dusty air and dusty O_2 is plotted in Fig. 6. For comparative analysis, τ_w and Q_w for air and O_2 having uniform properties are also presented. As it can be seen from Fig. 6(a), that the skin friction is higher for both gases with constant properties and it shows reduction when the physical properties are taken as temperature dependent. Particulary, this reduction is remarkable for contaminated O_2. The may happen because of the fact that, the air and O_2 get less dense and less viscous with respect to variation in

temperature, and ultimately, the frictional forces becomes less influential in the boundary layer region. While on the other hand, opposite behavior is recorded in the plots of rate of heat transfer (see Fig. 6(b)). Such change is expected, as we have taken the gases which contains the dust particles. When the thermophyical properties of such dusty gases are assumed to be temperature dependent, the dust particles inside the gases attains the thermal as well as kinetic energy from the base fluid. This energy acts as a supportive force for the particles movement and collision, which as a result, generate more heat inside the convective regime and consequently Q_w is intensified. Interestingly, the rate of heat transfer is more likely to be intensified for the case of air as compared to O_2, when the variable thermophysical properties are taken into account.

Fig. 7 is plotted to visualize the detailed scenario of velocity and temperature profiles of carrier and particle phases for different values of amplitude of wavy surface a. As it can clearly seen form Fig. 7(a), that the velocities for both phases decreases significantly for non-zero values of amplitude of wavy surface a. Such behavior is expected, because when amplitude of the wavy surface increases, the air particulate suspension between crust and trough of the waves undergoes more resistance to flow and hence fluid velocity decreases. As, flat surface $a = 0$ offers no resistance to flow and the velocities for both phases of the suspension are maximum for flat surface and quickly attains its asymptotic value in the boundary layer region. However, the parameter a has reverse affect on temperature profile (see Fig. 7(b)). This may happens due to the fact that, the dust particles near the surface attains the thermal energy from the hotter surface of large amplitude and ultimately give rise to the temperature of dusty fluid in whole convective regime.

Representative velocity profiles and temperature profiles for carrier as well as dusty phase under the effect of variable gas properties parameters n_μ and n_λ are plotted in Fig. 8. As it can be seen from Fig. 8 (a), that the air with uniform thermophysical properties (i.e, $n_\mu = n_\lambda = 0.0$) acts like a supportive driving force that accelerates the air particulate suspension flow, and, as a result, the velocity for both phases, (U, U_p), within the boundary layer increases significantly. The plots for velocity profiles for both, carrier as well as particle phase, quickly attains its asymptotic value when the gas with uniform properties is penetrated into the mechanism. Further it is seen from Fig. 8(b) that the temperature profiles for both phases, (Θ, Θ_p), increases with increase in n_μ and n_λ. Since the gases are more sensitive to the changes in the temperature, so the temperature-dependent physical characteristics of the gas are responsible for this behavior as they causes an increment in temperature of the gas for both phases near the axis of the flow.

4 Conclusion

In this paper, the behavior of natural convection flow of two-phase dusty gas with variable thermophysical properties is analyzed along a vertical wavy heated plate. The nonlinear system of boundary layer equations are iteratively solved step-by-step by using implicit finite difference method along with the tri-diagonal solver. Computational results are shown for the physical quantities, namely, skin friction coefficient, rate of heat transfer coefficient, velocity and temperature profiles. The solutions are established for a range of physically important parameters which emerge from the mass concentration of dust particles and the variable thermophysical properties of the gas together with the sinusoidal wave form geometry. The solutions show some features which are not encountered in the flows where

thermophysical properties of the gases are taken as constant. It is found that the effect of temperature-dependent properties together with the particle loading parameter on wall heat transfer rate is more prominent than that of wall shear stress. Besides, the rate of heat transfer varies periodically in the direction of ξ and is smaller for a wavy surface ($a \neq 0$) than that corresponding to a flat surface ($a = 0$). From this analysis, it is also observed that mass concentration parameter, D_ρ, extensively promotes the rate of heat transfer whereas the variable thermophysical properties parameters n_μ and n_λ has pronounced effect in reduction of skin friction within the boundary layer region.

References

[1] Sparrow, E. M., Gregg, J. L., The variable fluid property problem in free convection, *Trans. ASME*, **80**, 1958, 879-886.

[2] Brown, A., The effect on laminar free convection heat transfer of temperature dependence of the coefficient of volumetric expansion, *J. Heat Transfer*, **97**, 1975, 133-135.

[3] Gray, D. D., Giogini, A., The validity of the Boussinesq approximation for liquids and gases, *Int. J. Heat Mass Transfer*, **19**, 1977, 545-551.

[4] Clausing, A. M., Kempka, S. N., The influences of property variations on natural convection from vertical surfaces, *J. Heat Transfer*, **103**, 1981, 609-612.

[5] Gebhart, B., Natural convection flow, instability, and transition, *J. Heat Transfer*, **91**, 1969, 293-309.

[6] Eckert, E. R. G., Drake, R. M., Analysis of Hear and Mass Transfer. McGraw-Hill, New York, 1972.

[7] Shang, D. Y., Wang, B. X., Effect of variable thermophysical properties on laminar free convection of gas, *Int. J. Heat Mass Transfer*, **33**, 1990, 1387-1395.

[8] Hisenrath, J., Tables of thermodynamic and transport properties, *National Bureau of Standards*, 1955.

[9] Rudinger, G., Fundamentals of gas-particle flow, Elsevier Scientific Publishing Co., Amsterdam, 1980.

[10] Farbar, L., Morley, M. J., Heat transfer to flowing gas-solid mixtures in a circular tube, *Ind. Eng. Chem.*, **49**, 1957, 1143-1150.

[11] Marble, F. E., Dynamics of a gas containing small solid particles, combustion and propulsion, 5th AGARD colloquium, Pergamon press, 1963.

[12] Singleton, R. E., Fluid mechanics of gas-solid particle flow in boundary layers, Ph.D. Thesis, California Institute of Technology, 1964.

[13] Michael, D. H., Miller, D. A., Plane parallel flow of a dusty gas, *Mathematica*, **13**, 1966, 97-109.

[14] Saffman, P. G., On the stability of laminar flow of a dusty gas, *J. Fluid Mech.*, **13**, 1962, 120-128.

[15] Michael, D. H., The steady motion of a sphere in a dusty gas,*J. Fluid Mech.*, **31**, 1968, 175-192.

[16] Datta, N., Mishra, S. K., Boundary layer flow of a dusty fluid over a semi-infinite flat plate, *Acta Mech.*, **42**, 1982, 71-83.

[17] Agranat, V. M., Effect of pressure gradient of friction and heat transfer in a dusty boundary layer, *Fluid Dyn.*, **23**, 1988, 729-732.

[18] Roopa, G. S., Gireesha, B. J., Bagewadi, C. S., Numerical investigation of mixed convection boundary layer flow of a dusty fluid over an vertical surface with radiation, *Afr. Math.*, **24**, 2013, 487-502.

[19] Siddiqa, S., Hossain, M. A., Saha, S. C., Two-phase natural convection flow of a dusty fluid, *Int. J. Numer. Method*, **25**, 2015, 1542- 1556.

[20] Yao, L. S., Natural convection along a vertical wavy surface, *J. Heat Transfer*, **105**, 1983, 465-468.

[21] Moulic, S. G., Yao, L. S., Natural convection along a wavy surface with uniform heat flux, *J. Heat Transfer*, **111**, 1989, 1106-1108.

[22] Rees, D. A. S., Pop, I., Free convection induced by a vertical wavy surface with uniform heat flux in a porous medium, *J. Heat Transfer*, **117**, 1995, 545-550.

[23] Hossain, M. A., Pop, I., Magnetohydrodynamic boundary layer flow and heat transfer on a continuous moving wavy surface, *Arch. Mechanics*, **48**, 1996, 813-823.

[24] Hossain, M. A., Rees, D. A. S., Combined heat and mass transfer in natural convection flow from a vertical wavy surface, *Acta Mechanica*, **136**, 1999, 133-141.

[25] Siddiqa, S., Hossain, M. A., Saha, S. C., Natural convection flow with surface radiation along a vertical wavy surface, *Numerical Heat Transfer, Part A: Applications*, **64**, 2013, 400-415.

[26] Molla, M. M., Hossain, M. A., Gorla, R. S. R., Radiation effects on natural convection boundary layer flow over a vertical wavy frustum of a cone, *Proc. IMechE Part C: J. Mechanical Engineering Science*, **223**, 2009 1605-1614.

[27] Siddiqa, S., Hina, G., Begum, N., Saleem, S., Hossain, M. A., Gorla, R. S. R., Numerical and analytical solution of nanofluid bioconvection due to gyrotactic microorganisms along a vertical wavy cone, *Int. J. Heat Mass Transfer*, **101**, 2016, 608-613.

[28] Siddiqa, S., Begum, N., Hossain, M. A., Radiation effects from an isothermal vertical wavy cone with variable fluid properties, *Appl. Math. Comput.*, **289**, 2016, 149-158.

[29] Siddiqa, S., Abrar, M. N., Awais, M., Hossain, M. A., Dynamics of two-phase dusty fluid flow along a Wavy Surface, *Int. J. Nonlin. Sci. Num.*, **17**, 185-193.

[30] Siddiqa, S., Begum, N., Hossain, M. A., Massarotti, N., Influence of thermal radiation on contaminated air and water flow past a vertical wavy frustum of a cone, *Int. Commun. Heat Mass*, **76**, 2016, 63-68.

[31] Apazidis, N., Temperature distribution and heat transfer in a particle-fluid flow past a heated horizontal plate, *Int. J. Multiphase Flow*, **16**, 1990, 495-513.

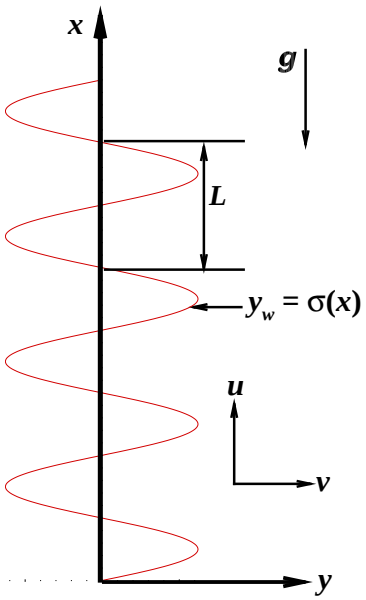

Fig. 1 Schematic of the problem.

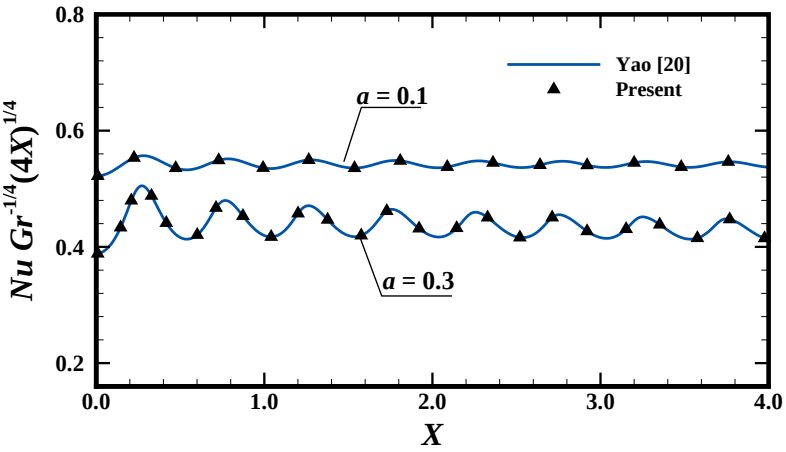

Fig. 2 Local Nusselt number coefficient for $a = 0.1, 0.3$, while Pr $= 1.0$, $D_\rho = \alpha_d = 0.0$ and $\lambda = n_\mu = n_\lambda = 0.0$.

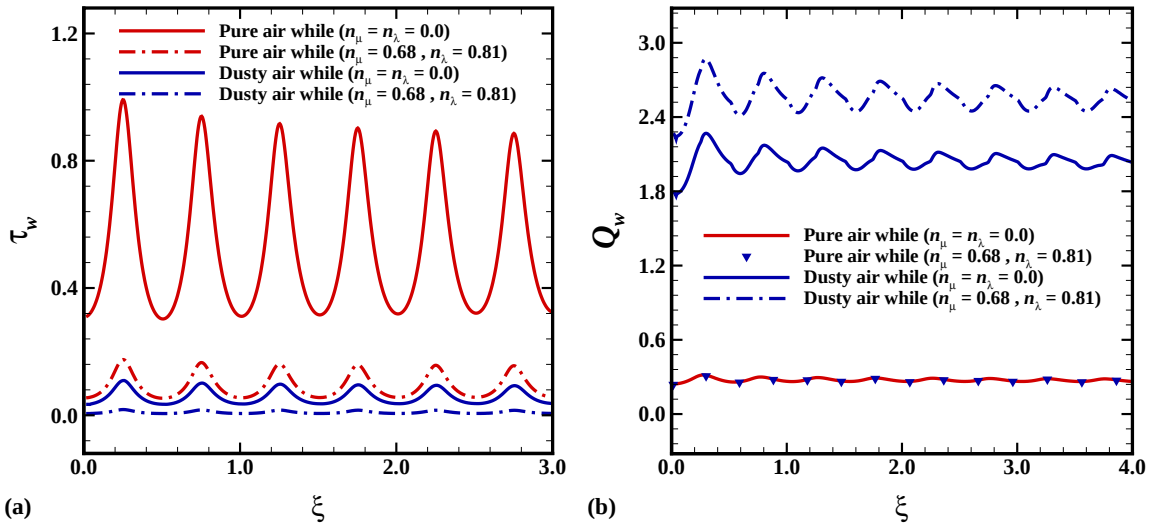

Fig. 3(a) Skin friction and (b) Rate of heat transfer coefficients for Air (Pr $= 0.7, n_\mu = (0.0, 0.68), n_\lambda = (0.0, 0.81), \lambda = (0.0, 1.0)$) while $D_\rho = (0.0, 10000.0)$, $\gamma = 0.45$, $\alpha_d = 1.0$ and $a = 0.3$.

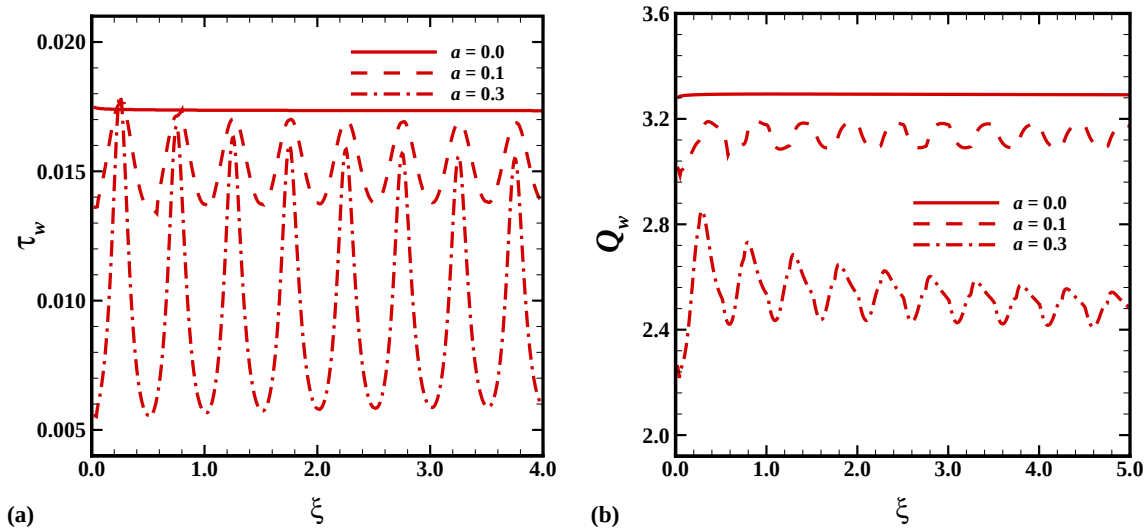

Fig. 4(a) Skin friction and (b) Rate of heat transfer coefficients for $a = (0.0, 0.1, 0.3)$ **while Pr** $= 0.7$**,** $n_\lambda = 0.81$**,** $n_\mu = 0.68$**,** $\lambda = 1.0$**,** $D_\rho = 10000.0$**,** $\gamma = 0.45$ **and** $\alpha_d = 1.0$**.**

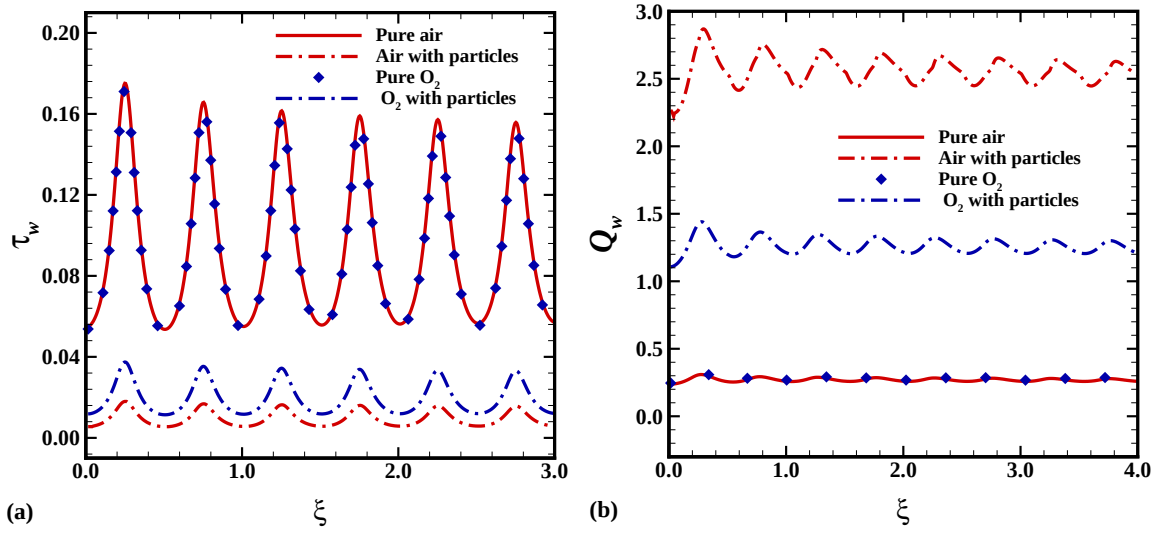

Fig. 5 Comparison of (a) Skin friction coefficients and (b) Rates of heat transfer of Air $(\mathbf{Pr} = 0.7, n_\mu = 0.68, n_\lambda = 0.81, D_\rho = (0.0, 10000.0))$**,** $\mathbf{O}_2(\mathbf{Pr} = 0.733, n_\mu = 0.694, n_\lambda = 0.86, D_\rho = (0.0, 500.0))$ **while** $\lambda = 1.0$**,** $\alpha_d = (0.0, 1.0)$**,** $\gamma = 0.45$ **and** $a = 0.3$**.**

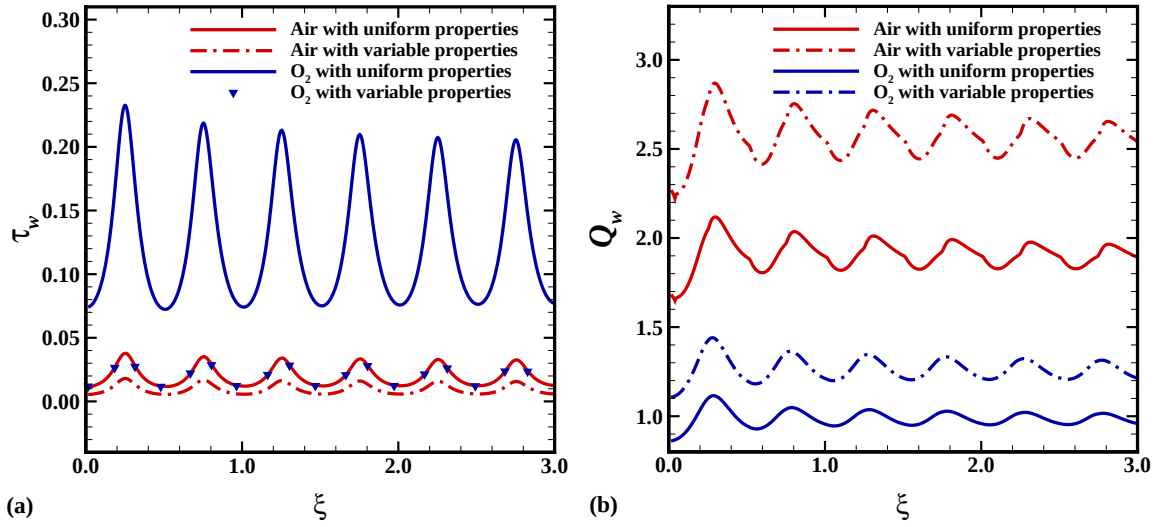

Fig. 6(a) Skin friction and (b) Rate of heat transfer coefficients of Air $(\mathbf{Pr} = 0.7, n_\mu = (0.0, 0.68), n_\lambda = (0.0, 0.81), D_\rho = 10000.0)$ **and** $O_2(\mathbf{Pr} = 0.733, n_\mu = (0.0, 0.694), n_\lambda = (0.0, 0.86), D_\rho = 500.0)$ **while** $\lambda = (0.0, 1.0)$**,** $\gamma = 0.45$**,** $\alpha_d = 1.0$ **and** $a = 0.3$**.**

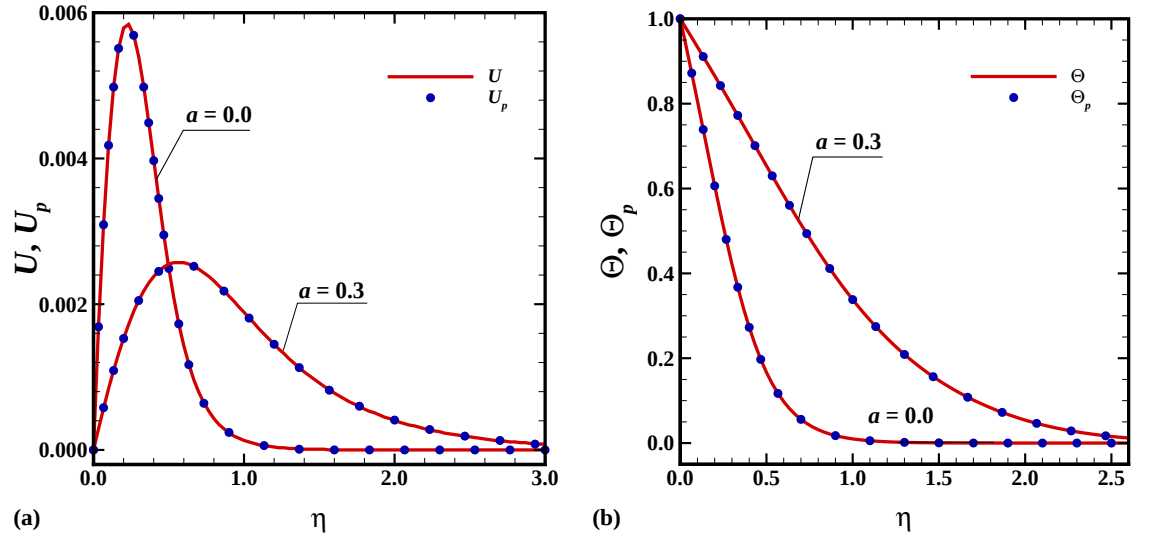

Fig. 7(a) Velocity and (b) Temperature profiles for for $a = (0.0, 0.3)$ **while** $\mathbf{Pr} = 0.7$**,** $n_\lambda = 0.81$**,** $n_\mu = 0.68$**,** $\lambda = 1.0$**,** $D_\rho = 10000.0$**,** $\alpha_d = 1.0$**,** $\gamma = 0.45$ **and** $\xi = 10.0$**.**

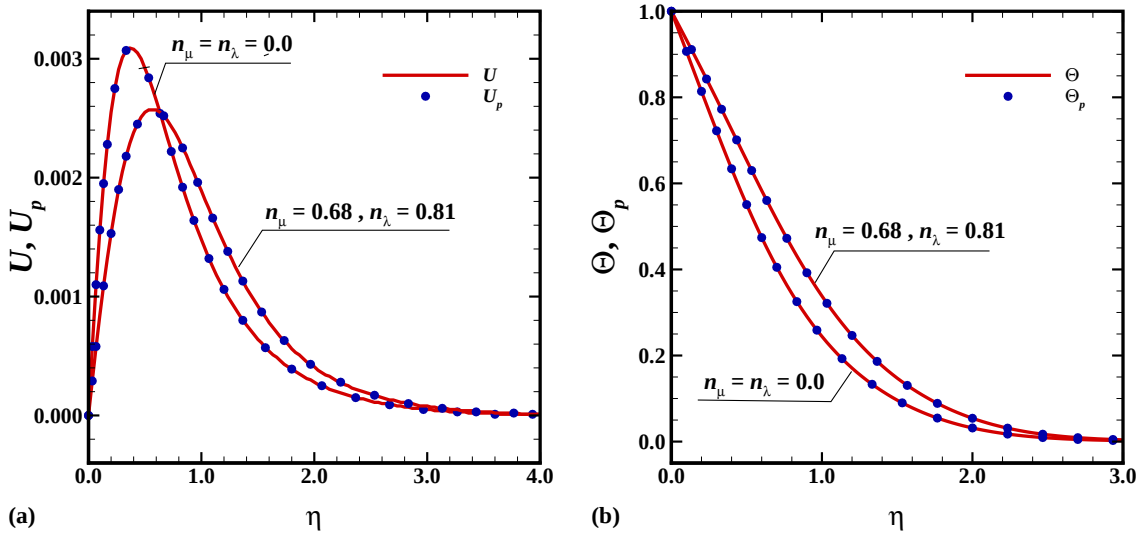

Fig. 8(a) Velocity and (b) Temperature profiles of Air ($\mathbf{Pr} = 0.7, n_\mu = (0.0, 0.68), n_\lambda = (0.0, 0.81), \lambda = (0.0, 1.0)$) **while** $D_\rho = 10000.0$**,** $\alpha_d = 1.0$**,** $\gamma = 0.45$ $a = 0.3$ **and** $\xi = 10.0$**.**